INSTRUMENTED CRANK SLIDER MECHANISM FOR VALIDATION OF A COMBINED FINITE ELEMENT WEAR MODEL

Nathan A. Mauntler[1], Nam-Ho Kim[1], W. Gregory Sawyer[1] and Tony L. Schmitz[1]
[1]Department of Mechanical and Aerospace Engineering
University of Florida
Gainesville, Florida, United States

INTRODUCTION

Software currently being produced at the University of Florida is incorporates traditional wear models into finite element analyses. This Coupled Evolution Wear Model (CEWM) uses the finite element method and generic material wear rates to continuously update contact pressures and geometry. This software package can be used to predict wear evolution, degradation of precision motion, and ultimately the end of a joint's useful life. Whereas traditional wear models do not account for changes in load profile due to changes in geometry, the CEWM iteratively updates material loss, shape, and pressure distributions to more realistically predict how a joint wears. This model has already been adapted and validated for several scenarios including a block on ring and the human knee [1,2]. Ultimately this software package will be available to designers in order to predict the influence of wear on the performance of moving parts over the course of their useful lives.

Recently the CEWM has been adapted to model a crank slider mechanism, where the integrity of the joint between the crank and connector rod can influence the ability to accurately control the location of a follower link. In order to validate the CEWM in this scenario, a crank slider tribometer is used to run controlled wear tests at the crank-connector rod joint (Fig. 1).

MECHANICAL DESIGN

The design of the tribometer is centered around the isolating friction, wear, and error motions to the joint of interest as much as possible.

Motion Generation

Motion of the crank slider is driven by a high-stiffness block spindle powered by a ¾ HP DC motor. This motor is elevated to the same height as the follower joint to minimize out-of-plane moments. A flywheel with 0.0847 kg-m^2 mass moment of inertia can be attached to the spindle to help maintain a constant velocity.

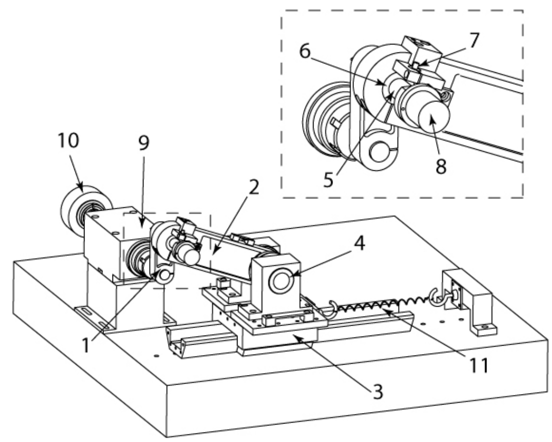

FIGURE 1. Crank slider tribometer (1) Crank arm (2) Follower arm (3) Slide (4) Thrust bushing (5) Instrumented pin (6) Bushing (7) Capacitance probe (8) Slip ring (9) Spindle (10) Encoder (11) Loading spring

The crank and follower arm are both machined from aluminum and pocketed to reduce weight. The crank is clamped to the spindle shaft at one end and to an instrumented pin at the other end. The pin is then free to rotate within a wearing bushing which is clamped in the follower arm. The follower arm is then constrained to in-plane rotations by two thrust air bushings. These bushings are mounted in pillow blocks which are in turn bolted to a dovetail air bearing stage. Both the thrust bushings and dovetail slide are constructed from porous carbon air bearings to minimize error motions while maintaining a high level of joint stiffness. All of the structural components of the tribometer are bolted to a granite plate.

Instrumentation

Forces transmitted through the joint of interest are measured via a load cell built into a steel pin (Fig. 2). Two full-bridge arrays of strain gages mounted to a necked-down portion of the pin monitor transverse loads while cancelling out bending stresses. The necked portion of the pin, along with a hollow cross section, also serve to localize the strain to the region where the gages are attached. A milled face allows repeatable orientation of the pin with respect to the crank arm. A slip ring mounted to the free end of the pin allows power and signals to be transmitted to and from the strain gages. The load cell is dead-weight calibrated, has a full scale capacity of 400 N and a resolution of 2 N.

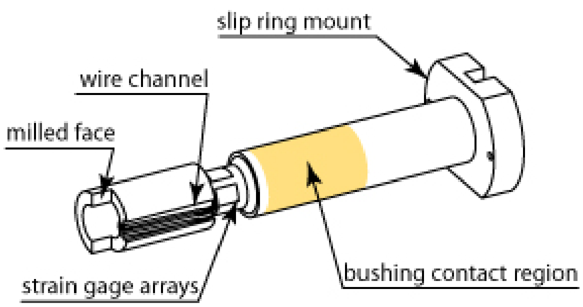

FIGURE 2. The pin at the joint of interest also serves as a load cell to measure transverse loads during testing.

Simultaneously, two orthogonally mounted capacitance probes monitor the position of the pin relative to bushing (Fig. 3). These probes are clamped to the follower arm and are electrically insulated by polymer bushings. Additionally, the pin, as the target, is electrically grounded.

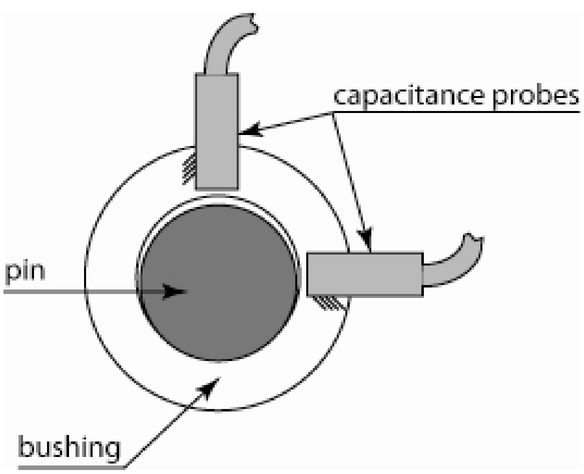

FIGURE 3. Orthogonally mounted capacitance probes monitor the position of the pin with respect to the bushing.

Additionally, the angular position of the crank is measured by a hollow shaft incremental encoder attached to the spindle shaft.

Load Profile

In addition to the inertial load of the slide and follower arm, the load profile seen by the pin-bushing joint can be adjusted in two ways. First, a spring can be added to the air bearing stage to provide a positional dependence to the load profile. Also, up to 10 kg of additional mass can be added to the stage. Adding mass to the stage influences the load profile as a function of both acceleration and position.

DATA ACQUISITION

Data from the load cell, capacitance probe, and encoder are collected simultaneously as waveforms. Typically, a packet of data is acquired once per revolution at a pre-specified sampling rate, depending on the crank speed. For each channel, the maximum value, minimum value, and root mean square of the data are then recorded to show broad trends over many cycles at a glance (Fig. 4).

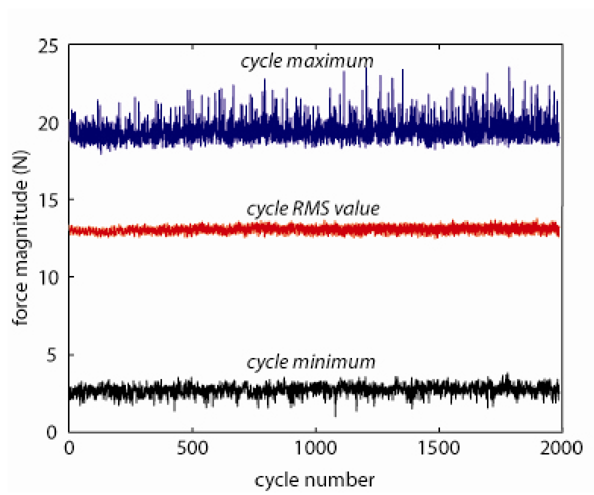

FIGURE 4. Force magnitude extrema plotted as a function of cycle number. Variations in the cycle maximum force value can be seen to increase as the test progresses.

Additionally, whole cycles of data from each channel are periodically saved. Force and displacement signals can then be plotted against the crank position to observe the evolution of the force profile and bushing geometry (Fig. 5). This also allows events observed in the force data to be directly correlated to events in the displacement data.

-

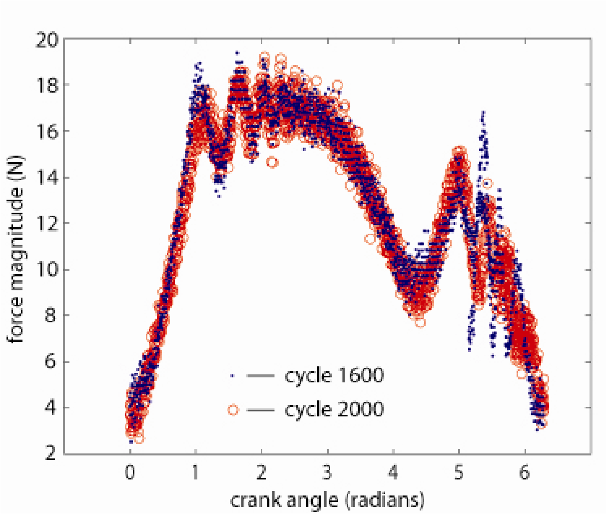

FIGURE 5. Force magnitude data from two cycles. The load profile can be seen to evolve in the severity of the dynamic forces.

FUTURE WORK

In the near future, whole tests will be run in which bushings are worn from their original state until the range capacity of the capacitance probes have been met. The results from these tests will then be compared to CEWM simulations using the same initial conditions.

REFERENCES

[1] Bei, Y. et al. The Relationship Between Contact Pressure, Insert Thickness, and Mild Wear in Total Knee Replacement. Computer Modeling in Engineering and Science. 2004; 6: 145-152.

[2] Kim, N.H. et al. Finite Element Analysis and Validation of Metal/Metal Wear in Oscillatory Contacts. Wear. 2005; 258: 1787-1793.